NIR photopolymer for micro-optics applications

Ihab Dika, Frédéric Diot, Véronique Bardinal, Jean-pierre Malval, Carole Ecoffet, Aurélien Bruyant, David Barat, Benjamin Reig, Jean-baptiste Doucet, Thierry Camps, et al.

DOI: 10.1002/
Article type: Full Paper

NIR photopolymer for micro-optics applications

*Ihab Dika, Frédéric Diot, Véronique Bardinal, Jean-Pierre Malval, Carole Ecoffet, Aurélien Bruyant, David Barat, Benjamin Reig, Jean-Baptiste Doucet, Thierry Camps and Olivier Soppera**

Ihab Dika, Frédéric Diot, Jean-Pierre Malval, Carole Ecoffet, Olivier Soppera
Université de Haute-Alsace, CNRS, IS2M UMR 7361, F-68100 Mulhouse, France
Université de Strasbourg, France
* corresponding author : olivier.soppera@uha.fr

David Barat, Benjamin Reig, Jean-Baptiste Doucet, Thierry Camps,Véronique Bardinal,
LAAS CNRS,7 avenue du colonel Roche, F-31077 Toulouse, France
Université de Toulouse ; UPS, INSA, INP, ISAE ; LAAS ; F-31077 Toulouse, France

Aurélien Bruyant,
Institut Charles Delaunay, UMR CNRS 6281, LNIO, Université de Technologie de Troyes,
12 rue Marie Curie - BP 2060 - 10010 Troyes Cedex, France

Keywords. Photopolymer, microlenses, waveguide, optical fiber, NIR

Near infrared (NIR) activable photopolymers suitable for versatile fabrication of micro-optical elements were developed. The first main objective of this paper is to show that these new photopolymers can be used for microfabrication and investigate the parameters governing the microfabrication process. The impact of photonic, physico-chemical and chemical parameters is discussed. High quality microstructures with a good control over their size and shape are demonstrated. The second main objective is to show practical examples of microlenses and waveguides implemented on single core and multiple core optical fibers, VCSELs, and glass slides are then presented. The NIR photosensitivity of this negative tone photoresists allows using the device source itself as to start the crosslinking process, which constitutes a convenient approach for micro-optics self-positioning on NIR sources and justifies the interest of such NIR photopolymer for the fabrication micro-optical elements and optical interconnects.

1. Introduction

Fabrication and integration of micro-optical elements (microlenses, microprisms, microgratings) and optical interconnects (waveguides) is one of the key-step enabling the emergence of new optical integrated devices.[1,2] In this context, NIR light sources are quite strategic for many photonic applications, ranging from high speed optical interconnects to instrumentation, printing and sensing. The huge success of these near infra-red sources, such as vertical-cavity surface-emitting lasers (VCSELs) is due to their unique properties, such as high compactness, low electrical consumption, parallel operation and on-wafer test capabilities, as well as high bandwidth modulation properties and high beam quality. However, for developing applications based on these light sources, micro-optical components are needed for beam shaping, redirecting or coupling.

Most of the current fabrication techniques are based on classical photolithography approaches and are thus intrinsically limited to 2D optical components. Novel fabrication techniques with various complexity and versatility have been proposed like thermal reflow process,[3] deep lithography with protons,[4] LIGA,[5] photolithography,[6] cantilever-based spotter,[7] UV imprint,[8] laser ablation,[9] direct writing by ion beam,[10] or laser[11]… Two-photon stereolithography is also a very performing technique for 3D microfabrication[12] but presents some inherent drawbacks on complex substrates, high cost equipment and low fabrication rates, which makes this technique still unsuitable for industrial applications in its current state of development. In addition, most of these techniques are limited in terms of materials, they usually require complex setup and one of the main difficulties is linked to the precise alignment of the micro-optical element with the light source in the optical pathway. [13]

To cope with these limitations, self-guided photopolymerization has been proposed a few years ago.[14] This method relies on the use of the optical source itself or on the light emerging from an optical element to build the new optical microsystem (**Figure 1**). The physical principle used here is to take advantage of the increase of the refractive index during polymerization to build a waveguide inside a photopolymerizable medium.[15,16,17] Thus, a lateral confinement of the electromagnetic field can be obtained on large distances, up to hundreds of microns or millimeters.

One of the major advantages of this technique in the frame of micro-optical element implementation is to inherently guarantee a perfect alignment of the optical element with the light source, which is one of the most challenging aspects when dealing with miniaturized devices and with collective fabrication. Thanks to the wide possibilities of macromolecular science, a wide variety of properties can be obtained by tuning the monomers and doping the polymer (fluorescent, photochromic, electrochromic...).

The investigation of self-guided photopolymerization was carried out using visible or UV light, both theoretically and experimentally. [18, 19, **Erreur ! Source du renvoi introuvable.**, 20, 21, **Erreur ! Source du renvoi introuvable.**, **Erreur ! Source du renvoi introuvable.**]

The concept has then been extended to NIR spectral range, which opens the possibility of integration of optical elements on VCSELs. This recent breakthrough relies on the development of new NIR sensitive photopolymers [25,26,27]. NIR photopolymers has been initially developed for graphic industry [28] and holography.[29] As light penetration is higher in NIR region than in the UV, there has been a renewed interest for these systems in the field of photocuring in depth [30,31]. Direct integration of microlenses on VCSELs was described in previous study and a first analyse of the effects of the photochemical and photonic parameters was conducted.[32]

In this work, we propose a NIR photopolymer destined at micro-optical applications. The critical parameters are : (i) photosensitivity in the NIR for efficient photopolymerization , (ii)

high absorption ability of the photoinitiator associated to a complete dye photobleaching after irradiation to provide a good initial confinement of light in the propagation direction and a transparency of the optical element at the operating wavelength after fabrication, (iii) low surface roughness and scattering for high transparency, (iv) good mechanical properties after NIR photopolymerization to allow the use of the material without any further process.

The first main objective of this paper is to show that this new photopolymer can be used for microfabrication and we investigated the parameters governing the microfabrication process. The impact of photonic, physico-chemical and chemical parameters is discussed. High quality microstructures with a good control over their size and shape are demonstrated.

The second main objective is to show practical examples of microlenses and waveguides implemented on single core and multiple core optical fibers, VCSELs, and glass slides are then presented. The NIR photosensitivity of this negative tone photoresists allows using the device source itself as to start the crosslinking process, which constitutes a convenient approach for micro-optics self-positioning on NIR sources.

2. Effect of photonic parameters

2.1 Specificity of the NIR photopolymer

NIR photopolymers were specifically designed to fulfill the requirements needed for microfabrication in this spectral range. A cyanine dye, namely the 1,1,3,3,3,3-Hexamethylindotricarbocyanine iodide ([$HITC^+$,I^-], denoted as HITC), was used as photoinitiator, with N-methyl diethanolamine (MDEA) as a co-initiator. HITC was chosen for its very strong absorptivity ($\varepsilon_{MAX} \geq 1 \times 10^5$ M^{-1} cm^{-1}) in the 700-900 nm range. Interestingly, the NIR dye bleaches during NIR irradiation, leading to a transparent material in NIR region

[26], which is obviously required for optical applications. The main processes of photochemical pathway involved in this material are depicted in **Figure 2**.

Compared to other free-radical photopolymerizable formulation sensitive to visible light (like Y-Eosin/MDEA or Methylen Blue/MDEA), the NIR sensitive systems present some particularities: the absorption of light From HITC ground state ($HITC^{+}$) leads classically to singlet excited species and subsequently to triplet excited ones by intersystem crossing but unlike other systems, MDEA can't react directly with the triplet state of HITC.[26] The production of reactive radicals implies subsequent reactions in which the excited triplet species can either react together (i.e. triplet-triplet annihilation) or with a dye at ground state (i.e. self-quenching). The resulting dication ($HITC^{2+}$) is then able to react with MDEA and produce the primary radicals that induce the free-radical polymerization of the acrylate monomers. This particular photochemical pathway has two consequences: i) at low triplet concentration (low light intensity), it allows a regeneration of excited HITC and ii) at high light intensity, the probability of reaction between two HITC molecules in triplet state is high and leads then to an annihilation of reactive species and inhibits the polymerization. In other words, unlike other photopolymer systems, high fluence is paradoxically unfavorable to polymerization process.

In parallel, low fluence regimes are usually not favorable for polymerization due to another molecular process called oxygen inhibition. Indeed, organic radicals are known to be very reactive towards molecular oxygen, leading to the creation of peroxo-radicals that are not reactive for further polymerization. In consequence, part of the radicals is killed by oxygen. It has to be emphasized that oxygen is always present in the starting monomer and the consumption of O_2 is a key step before polymerization can start. At low fluence, its consumption can be counterbalanced by diffusion of oxygen from non-illuminated area. Moreover, as the configuration used here is an open system, the possibility for oxygen to diffuse from the outer atmosphere can provide a continuous replenishment of oxygen. In this

case, polymerization is ineffective. The consequences of this singular molecular pathway have to be integrated in the microfabrication process to finely tune the light intensity and will be discussed later.

2.2. Influence of the photonic parameters on the photopolymer

Growing microtips at the end of an optical fiber was chosen as a reference setup to investigate the properties of the NIR photopolymer for microfabrication. **Figure 3** illustrates how intensity and dose (time x intensity) influence the shape of a microtip obtained by photopolymerization at the output of an optical fiber.

When considering a single row, the intensity is constant and the growth of the tip can be followed as a function of irradiation time (and dose). In a single column, the dose is constant, which allows to investigate the influence of fluence.

As expected, the length of the tip was increased with the received dose, until a plateau corresponding to the size of the photopolymer drop deposited at the end of the fiber. The time needed to grow the tip can be explained by the time needed to bleach the NIR dye through the drop. When the maximum length was reached, a slight enlargement of the diameter of the tip was observed. However, this enlargement is limited, demonstrating the efficient confinement of the light through the self-guiding process.

The impact of the intensity on the growth mechanism is more complex. Indeed, when considering a single column (e.g. a given dose), the evolution of the size of the tip was not monotone but an optimum intensity around 0.1 mW was clearly observed. As explained in the previous section and on **Figure 2** two phenomena can limit the efficiency of the initiating process: inhibition by oxygen for the lowest fluences and bimolecular reactions between excited states for high fluences. As a consequence, three regimes indicated by numbers on the side of **Figure 3** can be observed. For regime corresponding to intensities between 0.01mW

and 0.03 mW (1), the polymerization is controlled by oxygen inhibition and diffusion. As it can be seen, very small tips were obtained and the polymerization was completely inhibited when the intensity was lower than 0.01mW even for the longest irradiation times. In the intermediary regime (2 - intensities between 0.05 mW and 0.5 mW), the growth of the tips is mainly controlled by the light dose, which gives the maximum variation of shape when changing the irradiation time. At highest intensity (3 - above 1 mW), the polymerization efficiency dramatically drops down, due to the triplet-triplet annihilation. This regime is highly specific to the system used here and it was observed only because the density of energy is very high in this configuration, due to the very small surface of the laser beam emerging from the fiber (1 mW on 9 μm diameter roughly corresponds to 1.5 kW/cm^2).

All these distinctive regimes can be highlighted and rationalized by measuring the photopolymerization threshold as function of the NIR intensity. Indeed the photopolymerization energy threshold is defined here as the minimum dose required to observe the polymerization at the end of the fiber. When this value is reached, a tiny polymer part is observed at the end of the fiber. The resulted plot of energy threshold *vs.* NIR intensity is depicted in **Figure 4**.

This graph clearly confirms the three regimes described previously. In zone 1, governed by oxygen inhibition and diffusion, the threshold is gradually decreased when the light intensity (I) is increased. This predominant role of oxygen at low power was confirmed by the set of experiments depicted in **Figure S1** in the supporting information. The threshold was found independent of the light power at low power (in the range between 0.01 to 7 μW). In zone 2, the threshold is independent of I. Irradiation time and intensity are thus equivalent parameters and the dose (product of intensity by irradiation time) is the most relevant parameter. Finally, in zone 3, the unexpected apparent loss of polymerization efficiency is due to triplet-triplet annihilation, as discussed before.

Such data are of paramount importance for choosing the most adapted experimental conditions for microfabrication. Indeed, the most interesting conditions are the second regime, for which the shape of the microtips can be tuned with the largest dynamic.

3. Effect of chemical parameters

3.1 Effect of dye concentration

Beside the photonic parameters, the effect of the dye concentration has to be studied to fully describe the fabrication process. Experiments with various concentrations of HITC and laser power were carried out. The main results are plotted in **Figure 5**. This figure displays the images of microtips fabricated with various conditions and also, we plotted the tip volume versus the dose received by the photopolymer. The volume was evaluated from the microscopy images, assuming that the shape follows an ellipsoidal volume. In this case, the volume V is given by

$$V = \pi/6.D^2L \qquad (1)$$

where D is the diameter of the tip at its basis and L is the length.

Three intensities were used here: 0.02 mW corresponding to the regime 1 in the previous data set, 0.1mW for the regime 2 and 2 mW for high intensities (regime 3). Three concentrations of HITC were used (0.1%, 0.18% and 0.5%) and the concentration of MDEA was kept constant (4 wt. %).

At 0.02 mW (**Figure 5-a**), the increase of sensitivity of the photopolymer with the concentration of HITC is obvious and corresponds to an expected behavior since at higher concentrations, more reactive species are created and they can counterbalance the inhibitive effect of oxygen more efficiently. This behavior is clearly highlighted by the graph showing the polymerized volume versus the dose. A closer look to the dynamic of growth shows

another specificity of the high concentration system: whereas the volume of the tip is almost independent on the irradiation time at 0.18 % of HITC (a plateau is reached in the graph for 1 mJ), it is highly dependent on it at 0.5 %. This is attributed to the internal filter phenomenon. As the optical density of the formulation is higher for high dye concentration, the intensity drops down as a function of the distance from the output of the fiber. Once polymerization has occurred, the material is bleached and the light propagates further. Propagation of polymerization along the optical axis is thus governed by a progressive bleaching of the dye. This phenomenon can be very interesting for tailoring the lens height.

At moderate intensity (0.1 mW), the previous trend was confirmed, as shown in **Figure 5-b**. At moderate dye concentration (0.18%), a plateau is reached. The final polymerized volume is higher than for 0.02 mW. High dye concentration improved significantly the polymerization at low irradiation times and high absorption provokes a strong modification of the height of the lenses that is hardly achievable under such condition with lower dye concentration. In this case, the saturation of the polymerized volume for dose higher than 10 mJ is due to the limitation of the polymer tip maximum length that correspond to the thickness of the NIR photopolymer deposited at the end of the optical fiber. For the lowest dye concentration (0.10%), the polymerization can be triggered. A plateau is obtained that corresponds roughly to what is obtained for (0.02 mW-0.18%), which means that the important parameter is, as expected, the absorbed energy.

Interestingly, the results are quite different for the highest intensity (2 mW, **Figure 5-c**). Indeed, contrary to previous examples, polymerization at high dye content was found to be less efficient. On the photographs and on the graph, it is observed that the polymerization is not efficient for doses lower than 4 mJ. This observation confirms the assumption of high triplet-triplet annihilation for such system when a high concentration of reactive species is reached. Such conditions can be obtained either under high intensity and/or high dye concentration. This effect is thus to be considered with maximum care when designing a NIR

photopolymer. Another consequence is the low performance of the photopolymer for pulsed irradiation since the delivery of the energy within a limited time increases the probability of reaction between excited states. In particular, femtosecond laser irradiation was tested but such conditions were proved to be inadequate to trigger polymerization of such system (no polymerization), confirming the role of triplet-triplet annihilation for high reactive species concentration.

3.2 Effect of oxygen

As illustrated in **Figure 2**, oxygen may interact with the photopolymer at several levels of the photochemical process leading to desexcitation of excited states, in accordance with its reputation of free-radical polymerization inhibitor. Contribution of oxygen is of two origins: *i)* oxygen dissolved in the irradiated volume. It is generally considered that in acrylates, the equilibrium concentration of oxygen is around 3.10^{-3} mol/L^{-1}.[26]. It has to disappear before photopolymerization can start. The dose of energy necessary for its consumption is related to its concentration and is almost independent of the fluence. *ii)* oxygen diffusing from outside of the irradiation volume. Since the irradiation is limited to a small volume, it is compulsory to consider the oxygen diffusion towards the irradiated area from the rest of the photopolymer as well as the oxygen diffusing from the surrounding atmosphere. In this case, the contribution of the oxygen will highly depend on the relative rates of consumption and diffusion. Since the consumption process is directly related to the production of reactive species, a relation with light intensity is expected.

Figure 6 illustrates the role of oxygen on this molecular system. Under similar photonic conditions, the same experiments had been carried out under air and under a pure nitrogen atmosphere (N_2). **Figure 6-a** shows, for a given condition, how high the impact of oxygen can be: under the same photonic conditions a tip was obtained under the nitrogen atmosphere

whereas not a trace of polymer was observed in presence of oxygen. In other terms, the oxygen elimination leads to a significant decrease of the threshold energy and of the minimum intensity needed to start the polymerization. **Figure 6-b** exemplifies more completely this difference by comparing the dynamic of the tip growth under low intensity conditions. The photonic conditions (20 μW) were chosen to correspond to the region 1 defined in **Figure 4**, e.g. conditions governed by inhibition process. Thus, as expected, the inert atmosphere conditions lead to bigger tips, whatever the irradiation time, as shown in the graph (inset of Figure 6-b). Interestingly, the shape of the tips shows a significant difference from what was observed under aerated conditions. In particular, an increase of the diameter of the tips was observed. Such difference stresses out the high importance of oxygen to control and confine the polymerized volume. As shown in inset in Figure 6-b, the polymerized volume is almost constant in aerated conditions and significantly increasing with dose under nitrogen atmosphere. This compounds which is considered as a drawback in free-radical polymerization appears here as an interesting compound to control the extent of polymerization. A close look to the last tip of the series (450 sec) reveals an interesting shape with a diverging basis and a converging end. Such shape shows that the self-focusing effect due to the increase of the refractive index during polymerization allows counterbalancing the natural divergence of the light source. Such tip design appears as very interesting to minimize the optical losses at the basis of the tip. Further optical characterizations of such tip shapes are underway.

Finally, a series of tips made with the same dose (1 mJ) under air and nitrogen was done using different intensities ranging from 1 to 1000 μW. Under air atmosphere, a tip is obtained only for optimal photonic conditions (e.g. corresponding to medium intensity range). On the contrary, whatever the intensity, a tip was obtained in absence of oxygen. The relevant parameter for polymerization under inert atmosphere is thus the dose used whereas under air, the intensity also accounts for the final results.

3.3 Influence of the nature of the monomer

As a building block of the final material, the monomer is another key element in the formulation. It has a primary importance for final applications but plays also a role in the photochemical process. Acrylate monomers were considered here since these monomers are highly reactive towards radicals and a wide variety of commercial products are available to tune the refractive index and chemical function of the monomers. Among other parameters, the viscosity and functionality (number of acrylate functions per monomers) have a direct influence on microfabrication process. For this reason, we tested different monomers. Their molecular structures are given in **Figure S2** in the supporting information. However, these properties are not independent as shown in **Table S3**. Indeed, because the intermolecular forces increase with the increase of polar functions on the monomer, the viscosity increases with functionality. A first set of monomers was considered and for all of them, the threshold of polymerization as well as the optimum dose to obtain straight tips (when possible) was determined. The results are given in **Table S3**. For low viscosity and low functionality monomers (SR256, SR259, SR351), self-standing polymers could not be obtained, unlike the monomers with higher functionality (4 and 5). These series of tests suggest that increasing the functionality of the monomer is beneficial for the microstructuration process. To account for this behavior, two explanations can be suggested: first, the highest functionality favors the crosslinking density of the polymer network and improves the mechanical properties of the polymer network for a given conversion of the monomers. Secondly, the increased viscosity is due to an increase of the intermolecular forces that can also account for the cohesion forces within the polymer network. Another parameter to consider is the expected decrease of the diffusivity of oxygen in viscous medium, which limits the inhibition effect of oxygen as the viscosity of the monomer increases.

Thus, in order to decouple the impact of the functionality and viscosity, two sets of monomers with the same functionality and various viscosities were chosen. Results are presented in **Table S4**.

A wide range of viscosity is achievable with bifunctional monomers (from 10 to 10000 CPS). However, for the lowest viscosity monomers, no polymer could be observed on the optical fiber, meaning that the polymer network is too weak to resist to development. From 1600 CPS (SR349), the microfabrication is possible and the dose significantly decreases with increasing viscosity. Such an observation confirms that the viscosity of the monomer, that characterizes the intermolecular forces, is the parameter of importance for microfabrication. The same behavior was obtained for trifunctional monomers: no polymerization could be obtained with SR351 (106 CPS) whereas an efficient polymerization was obtained for PETA (800 CPS). For a given viscosity, the microfabrication is favored by an increase of the functionality, probably due to the higher probability to generate crosslinking nets within the polymer network.

In conclusion, trifunctional monomers with moderate viscosity are the most interesting. In particular, PETA was selected as a very good candidate for applications in microoptics.

4. Application to the fabrication of micro-optical elements.

4.1. Polymer microlenses on optical fibers

Microlenses integrated at the end of optical fibers are of highest interest due to their use in various applications such as coupling improvement between light sources and optical fibers, optical communication, optical fiber sensor and Near-Field Optical Microscope (SNOM) probes. Results shown in **Figure 3** illustrate the high flexibility of microtips shape achievable with the self-guiding approach. Tuning simple sets of parameters like the irradiation time and intensity of the actinic light allows generating a wide variety of microtips.

As an illustration, the radius of curvature of the tip extremity was deduced from the microscopy images and plotted in **Figure 7**. The radius of curvature can be tuned between 5 and 10 microns, which corresponds to focal length between 9.5 and 19 µm, assuming a refractive index of 1.52 in the polymer. Note that this value was taken as an average value for an organic polymer, that is usually admitted in such materials.[33,34,35] A precise evaluation of the polymer prepared in such conditions would be needed to give an accurate value of the refractive index, which could be done by modeling the beam propagation within the photoresist [18] or using tomographic microscopy. [36]

Moreover, this fabrication process is well-adapted to complex fibers. To demonstrate this possibility, a multicore fiber (7 cores) was used (**Figure 8**). By changing the coupling of the 780 nm light into the fiber, the cores can be selectively addressed. In **Figure 8-a**, the 7 cores were simultaneously excited during the irradiation process, leading to 7 similar microlenses that correspond to the extension of the 7 cores. In the inset of **Figure 8-a**, different excitation modes of the microlenses were used to illustrate the possibility to selectively excite part of the microlenses.

The cores can also selectively be addressed during the fabrication step, as shown in **Figure 8-b**. in this case, only 4 of the cores were excited. On this sample, another fabrication step was led by depositing a second time the photopolymer and exciting the other cores. Since different experimental conditions were used in this case, the new fabricated tips were longer. By adjusting the photonic parameters, the same range of geometry as described previously is accessible.

4.2. Microlenses on a transparent substrate

The self-guiding fabrication process can also be used to integrate microlenses or arrays of microlenses on transparent substrates as shown in **Figure 9**. In this case, the photopolymer is

not deposited on the fiber itself but on a transparent substrate and the light excitation is provided by the fiber placed in contact or near the substrate. The minimum distance between the end of the fiber that is used as a light source and the photopolymer corresponds to the thickness of the glass substrate (180 μm). A first set of experiment was done using this minimal distance. The results are displayed in **Figure 9-b**. Contrary to classical photolithography process, the self-guiding approach opens the door towards 3D microfabrication. The diameter of the lens is in all cases about 25 μm, as expected from the divergence of the light at the fiber output.

However, the radius of curvature of the microlens is almost independent of the irradiation time with such conditions. This parameter can be tuned by adjusting the distance between the end of the fiber and the glass substrate as shown in **Figure 9-c**. Due to the divergence of the optical fiber, the irradiation zone is enlarged by increasing the fiber-photopolymer distance. Since the power density is decreased by the same factor, it is normal to obtain a lower height. The profile of the lens is in this case remarkably smooth and quasi-Gaussian. Moreover, the radius of curvature of the center part of the lens is varying along a linear law, which is interesting for tuning the focal length of the polymer lens.

This result demonstrates the feasibility of remote micro-fabrication from an optical fiber. This could be also achieved from a VCSEL microsource in order to enlarge the possible range of microlens focal length. We show this possibility in **Figure 9-d**. In this example, a self-written microlens was fabricated on a SU8 spacer with a thickness of 100 μm. The VCSEL (emitting at 850 nm in this case) was used to fabricate the microlens so a perfect alignment of the microlens can be ensured without recourse to any sophisticated alignment system. We already demonstrated in previous works that microlenses prepared with a similar material present interesting optical properties by optical near-field and far-field analysis and FDTD simulations, showing the suitable optical properties of the material in the NIR range.[32,37] Other works are underway to further control the shape and thus focal length of such microlens

that would be of interest for VCSEL light collimating. This example also illustrates that the polymerization wavelength can be extended to 850 nm, thanks to the wide absorption spectrum of the dye.

4.3. Waveguides

As mentioned previously, the microlens tip is limited by the size of the photopolymer drop deposited at the end of the optical fiber. Thus, if the fiber is immersed in the photopolymer during irradiation, the fabrication of a waveguide is expected. **Figure 10-a** and **Figure 10-b** show the extension of the waveguide with irradiation time (0.1 mW). The growth of the waveguide with irradiation time is observed. The length follows a log law against the irradiation time, which is in accordance with first order bleaching kinetic of the NIR dye and Beer-Lambert law. In well-chosen irradiation conditions, a straight waveguide can be obtained (0.5 mW, 4s).

A close look to the micrographs given in **Figure 10-a** reveals singularities emphasized by red arrows. These constriction nodes along the waveguide are reproducible for given photonic parameters. More precisely, the position of the constriction node is constant for the different samples, showing that it is not an artifact. As shown in **Figure 10-c** and **Figure 10-d**, the position of the node depends linearly of the intensity of the laser. Interestingly, the diameter at the node also increases with intensity, leading to a waveguide more homogeneous in diameter. This observation is very important for fabrication purpose as usually, a constant diameter is wanted to optimize optical losses. Moreover, it appeared that a strong constriction node provokes an enlargement of the waveguide (**Figure 10-a**, 300 s), which is unwanted.

It also gives information on the origin of the node: the formation of the waveguide results from a competition between (i) the propagation of the polymerization linked to bleaching and (ii) the self-focusing effect due to the increase of the refractive index during polymerization.

At high power, **Figure 10-c** and **Figure 10-d** show that the prevailing effect is the propagation of polymerization along the optical axis, resulting in a constriction mode being repelled from the end of the fiber.

By controlling the irradiation conditions, it is possible to generate straight waveguides with constant diameter. Such waveguides have already demonstrated their interest for optical sensor and can be easily functionalized.[28,29,30]

5. Conclusion

A in depth investigation of a NIR photopolymer suitable for micro-optical applications was presented here. The photonic and physico-chemical conditions to obtain an efficient photopolymerization were defined. The photosensitivity of the photoresist at 780 nm is sufficient to obtain crosslinking with one photon irradiation with light sources that are commonly used in optical devices. Unexpected drop of photopolymerization efficiency at high fluence was shown and explained by triplet-triplet annihilation. Dependence of the free radical photopolymer to oxygen quenching at low fluence is observed. This photoresist is of high interest for applications in micro-optics as exemplified by fabrication of microlenses or waveguides. Further works are underway to extend the polymerization towards higher wavelengths of irradiation. In addition, such NIR photopolymer can find applications in other applications like rapid prototyping, optical data storage or laser direct writing of refractive or diffractive microelements triggered by NIR sources.

6. Experimental Section

The NIR photopolymer used for self-guiding microfabrication is composed of a NIR dye 1,1',3,3,3',3'-Hexamethylindotricarbocyanine iodide (HITC, typically 0.18 wt. %) associated

to a co-initiator N-methyl diethanolamine (MDEA, typically 4 wt. %) and an acrylate monomer polymerizing along a free-radial process under NIR irradiation. Acrylate monomers have been chosen for their high reactivity, high spatial resolution associated with a low surface roughness, good optical and mechanical properties after crosslinking.

A NIR laser diode emitting at 780 nm purchased from Sanyo (80 mW) was used as excitation source. The laser beam was injected into a single-mode optical fiber (SMF-28e from Corning, core Ø: 9 μm) using an objective with a numerical aperture of 0.4. To create microlenses, a droplet of the photopolymer was deposited on the other the side of the fiber by dipping the end of the fiber into the photopolymer. The capillarity effect ensures the formation of droplet with a reproducible and similar size (40 μm radius). In the case of waveguide formation, the free end of the fiber was dipped in the photopolymer and NIR light was put on with the fiber immersed in the photopolymer. With such conditions, the extent of the waveguide is no longer limited by the size of the deposited photopolymer drop.

Microtips and waveguides were analyzed by optical microscopy and SEM.

Supporting Information
Supporting Information is available from the Wiley Online Library or from the author.

Acknowledgements

The French National Research Agency (ANR) is gratefully acknowledged for financial support (ANR-09-BLAN-0168-01) as well as Carnot institutes MICA and LAAS for NIR-CONNECT project.

Received: ((will be filled in by the editorial staff))
Revised: ((will be filled in by the editorial staff))
Published online: ((will be filled in by the editorial staff))

References

1. K. I. Kardosh, F. Rinaldi, R. Michalzik, *Elec. Letters*, **2006**, 42, 2.

2. R. Yang, W. Wang., S. Soper, *Appl. Phys. Lett*., **2005**, 86 166110.

3. Y. Hsiharing, C. Chao, M. Wei, C. Lin, *J. Micromechanics Microengineering*, **2004**, 14(8), 1197-1204.

4. H. Ottevaere, B. Volckaerts, M. Vervaeke, P. Vynck, A. Hermane, H. Thienpont, *Jap. J Appli. Phys.*, **2004**, 43(1), 5832-5839.

5. S. Dong, S.L. Hyun, B.K. Lee, S.Y. Sang, K. Tai Hun, S.S. Lee, *Polym. Engin. Sci.*, **2006**, 46(4), 416-425.

6. Y. Lu, C. Shaochen, *Appl. Phys. Lett.*, **2008**, 92(4).

7. V. Bardinal, E. Daran, T. Leïchlé, C. Vergnenègre, C. Levallois, T. Camps, V. Conedera, J. B. Doucet, F. Carcenac, H. Ottevaere, and H. Thienpont, *Opt. Exp.*, **2007**, 15(11), 6900-6907.

8. S. Kim, H. Kim, S. Kang, *Opt. Lett.*, **2006**, 31(18), 362-5.

9. S. Mihailov, S. Lazare, *Appl. Opt.*, **1993**, 32(31), 6211-6218

10. W.X. Yu, X.C. Yuan, *Opt. Exp.*, **2003**, 11(8), 899

11. C. Croutxé-Barghorn, O. Soppera, L. Simonin, D.J. Lougnot, *Adv. Mat. Opt. Electron.*, **2000**, 10, 25-38.

12. K.S. Lee, R.H. Kim, D.Y. Yang, S.H. Park, *Prog. Polym. Sci.*, **2008**, 33, 631-681.

13. P.I Dietrich, M. Blaicher, I. Reuter, M. Billah, T. Hoose, A. Hofmann, C. Caer, R. Dangel, B. Offrein, U. Troppenz, M. Moehrle, W. Freude, C. Koos, *Nature Photonics* **2018**, 12, 241.

14. R. Bachelot, C. Ecoffet, D. Deloeil, P. Royer, D.J. Lougnot, *Appl. Opt.* **2001**, 40, 5860.

15. K. D. Dorkenoo, F. Gillot, O. Cregut, Y. Sonnefraud, A. Fort, H. Leblond, *Phys. Rev. Lett.* **2004**, 93 (14), 143905(4).

16. O. Soppera, S. Jradi, D. J. Lougnot, *Journal of Polymer Science Part a-Polymer Chemistry* **2008**, 46, 3783.

17. S. Jradi, O. Soppera, D. J. Lougnot, R. Bachelot, P. Royer, *Optical Materials* **2009**, 31, 640.

18. A. A. Sukhorukov, S. Shoji, Y. Kivshar, *Journal of Nonlinear Optical Physics & Materials* **2002**, 11(4), 391.

19. O. Sugihara, H. Tsuchie, H. Endo, N. Okamoto, T. Yamashita, M. Kagami, T. Kaino, *IEEE Photonics Technology Letters* **2004**, 16(3), 804.

20. A. J. Jacobsen, W. Barvosa-Carter, S. Nutt, *Adv. Mater.* **2007**, 19, 3892.

21. A. J. Jacobsen, W. Barvosa-Carter, S. Nutt, *Acta Materialia* **2008**, 56, 2540.

22. C. P. Jisha, V. C. Kishore, B. M. John, V. C. Kuriakose, K. Porsezian, C. Sudha Kartha, *Applied Optics* **2008**, 47(35), 6502.

23. E. Tolstik, O. Romanov, V. Matusevich, A. Tolstik, R. Kowarschik, *Optics Express* **2014**, 22(3), 3228.

24. N. D. Dolinski, Z. A. Page, E. B. Callaway, F. Eisenreich, R. V. Garcia, R. Chavez, D. P. Bothman, S. Hecht, F. W. Zok, C. J. Hawker, *Adv. Mater.* **2018**, 1800364.

25. O. Soppera, C. Turck, D. J. Lougnot, *Optics Letters* **2009**, 34, 461.

26. I. Dika, J. P. Malval, O. Soppera, V. Bardinal, D. Barat, C. Turck, A. Spangenberg, A. Bruyant, *Chemical Physics Letters* **2011**, 515, 91.

27. C. Schmitz, B. Strehmel, *ChemPhotoChem*, **2017**, 1(1), 26.

28. B. Strehmel, T. Brömme, C. Schmitz, K. Reiner, S. Ernst, D. Keil, *Dyes and Chromophores in Polymer Science John Wiley & Sons Inc*. **2015**, 213-249.

29. P. Nagtegaele, T. V. Galstian, *Synthetic Metals* **2002**, 127, 85.

30. C. Schmitz, A. Halbhuber, D. Keil, B. Strehmel, *Prog Org Coat* **2016**, 100, 32-46.

31. A.H. Bonardi, F. Dumur, T.M. Grant, G. Noirbent, D. Gigmes, B.H. Lessard, J.P. Fouassier, J. Lalevée, *Macromolecules*, **2018**, 51(4), 1314.

32. D. Barat, V. Bardinal, I. Dika, O. Soppera, P. Debernardi, A. Rumyantseva, B. Reig, M. Renault, T. Camps, A. Bruyant, J. B. Doucet, J. P. Malval, E. Daran, Optics Express 2012, 20, 22922.

33. K. Dorkenoo, A. J. Wonderen, H. Bulou, M. Romeo, O. Cregut, A. Fort, *Appl. Phys. Lett.* **2003**, 83, 2474.

34. C. Croutxe-Barghorn, O. Soppera, L. Simonin, D. J. Lougnot, *Advanced Materials for Optics and Electronics* **2000**, 10, 25.

35. H.I. El Ahrach, R. Bachelot, A. Vial, G. Lerondel, J. Plain, P. Royer, O. Soppera, *Phys Rev Lett* **2007,** *98* (10).

36. B. Simon, M. Debailleul, M. Houkal, C. Ecoffet, J. Bailleul, J. Lambert, A. Spangenberg, H. Liu, O. Soppera, O. Haeberlé, *Optica* **2017**, 4 (4), 460.

37. D. Barat, V. Bardinal, I. Dika, O. Soppera, A. Rumyantseva, B. Reig, M. Renault, A. Bruyant, J.B. Doucet, T. Camps, J.P. Malval, E. Daran, *Microelectronic Engineering* **2013**, 111, 204.

38. O. Frazao, P. Caldas, J. L. Santos, P. V. S. Marques, C. Turck, D. J. Lougnot, O. Soppera, *Optics Letters* **2009**, 34, 2474.

39. P. A. S. Jorge, C. Maule, O. Soppera, P. V. S. Marques, *IEEE Photonics Technology Letters* **2011**, 23, 492.

40. X. A. Ton, B. T. S. Bui, M. Resmini, P. Bonomi, I. Dika, O. Soppera, K. Haupt, *Angewandte Chemie-International Edition* **2013**, 52, 8317.

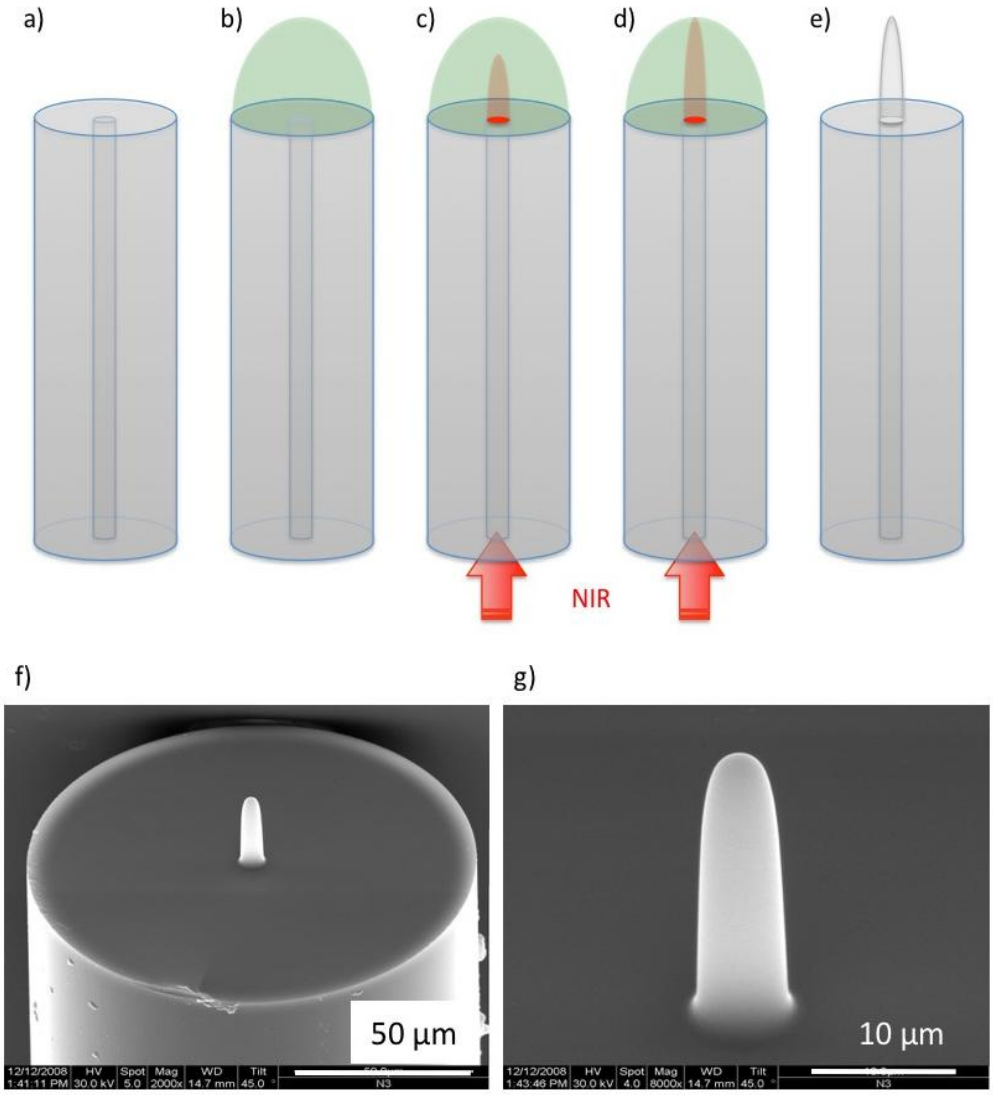

Figure 1. Schematic view of the self-guiding process on optical fiber: a) cleaved optical fiber; b) deposition of the NIR photopolymer on the extremity of the fiber; c) and d) irradiation by NIR light (780 nm) of the photopolymer through the fiber; e) polymerized tip. f) and g) are SEM images of microlenses created by this process.

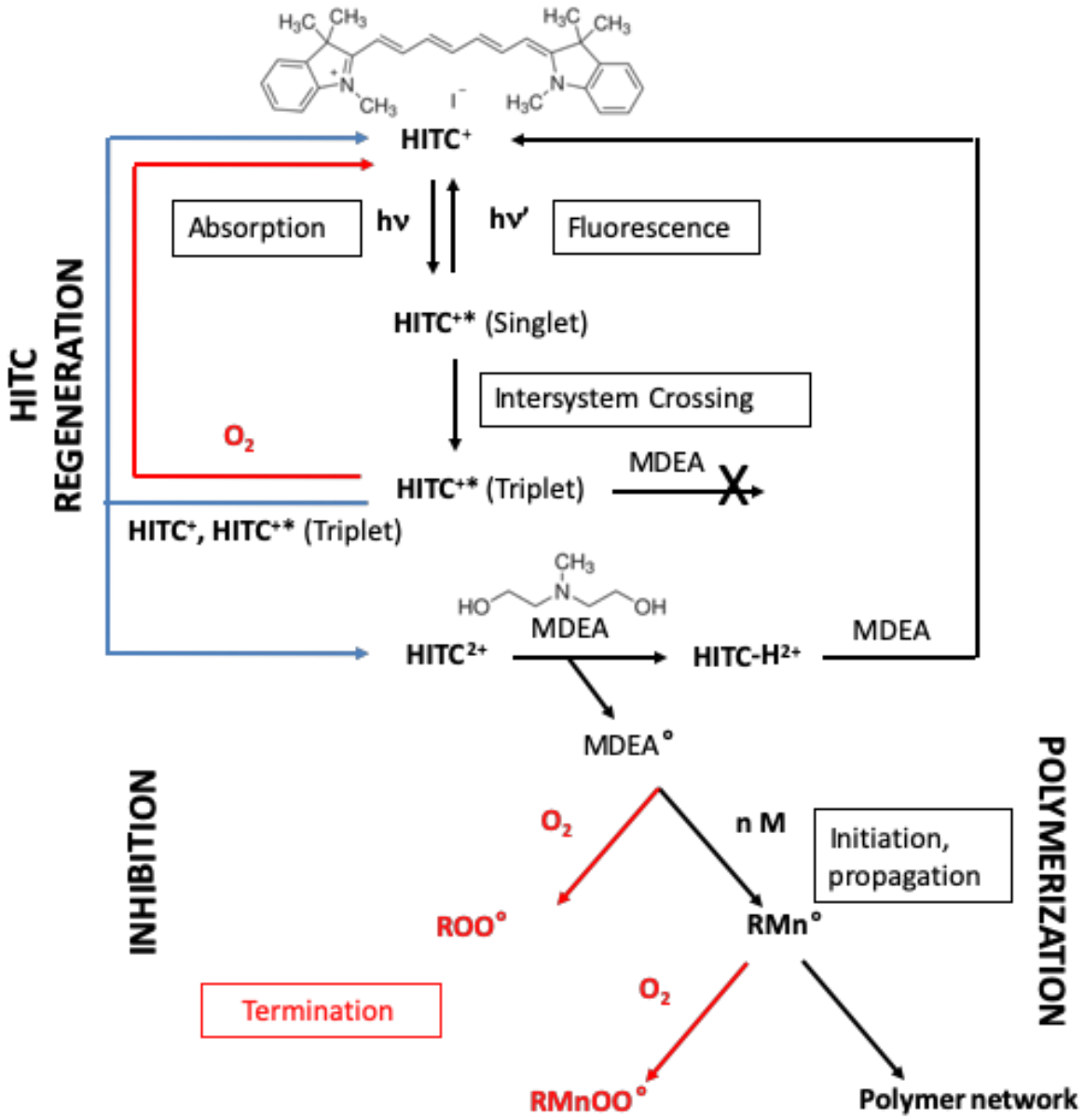

Figure 2. Molecular scheme for photopolymerization triggered by photoinitiating system (HITC/MDEA).

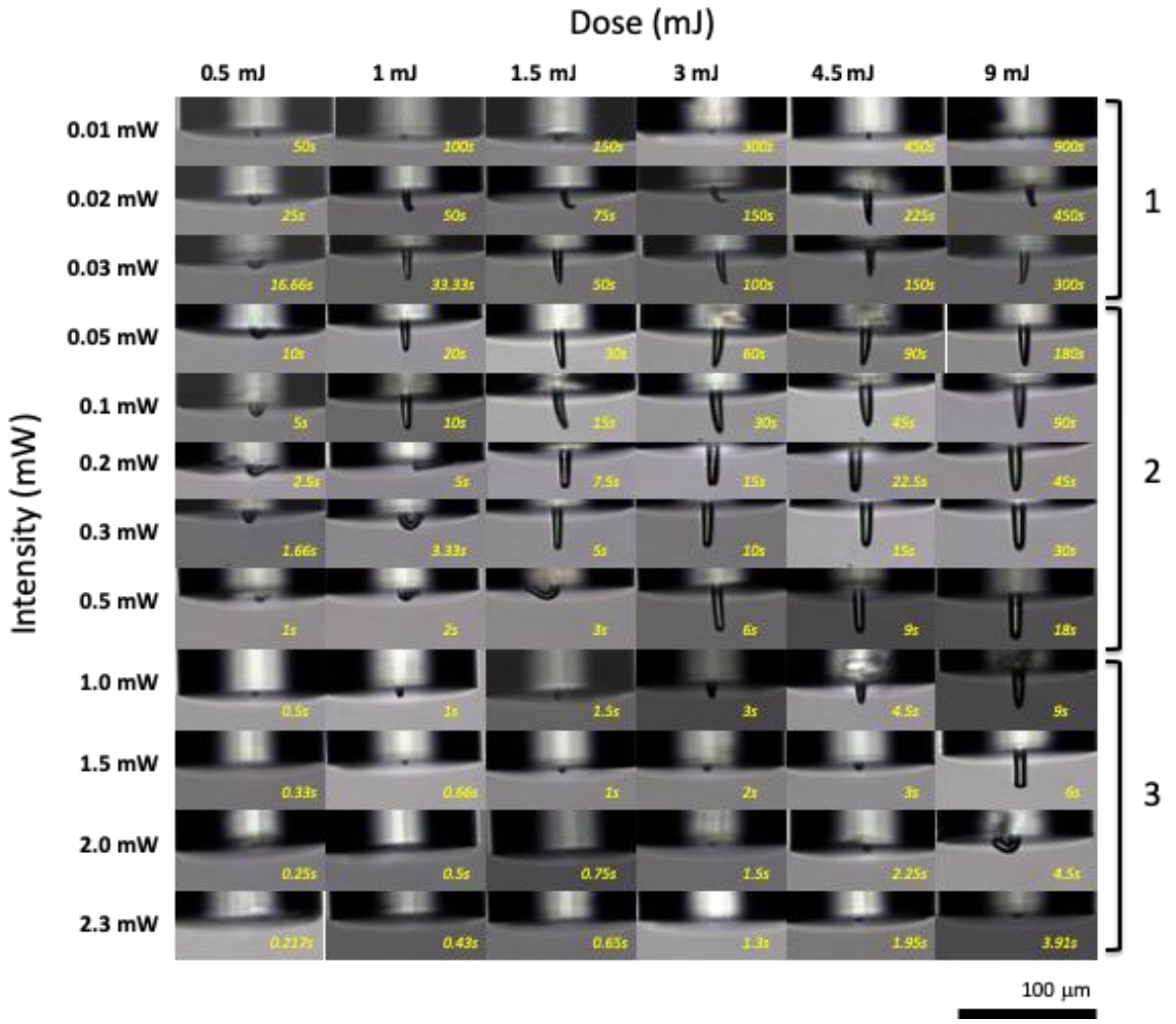

Figure 3. Effect of photonic parameters on photopolymerization at the end of optical fiber. Each row corresponds to a given intensity between 0.01 mW and 2.3 mW. Each column corresponds to a given dose between 0.5 mJ and 9 mJ. The irradiation time (in sec) used in each experiment is given in yellow.

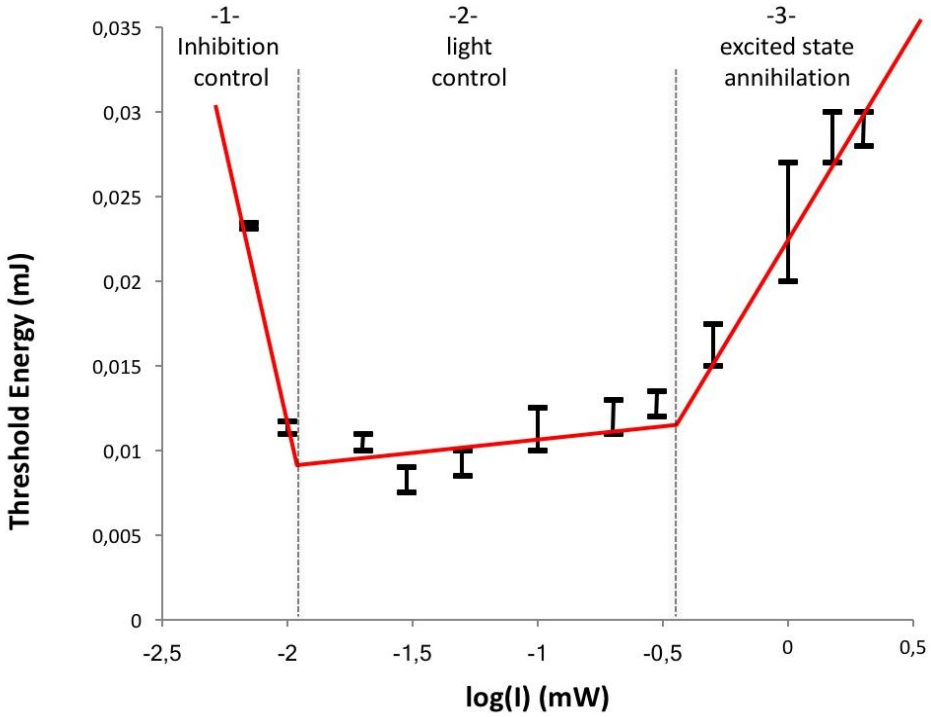

Figure 4. Threshold energy (mJ) as a function of the laser intensity (mW). The threshold energy is defined as the minimum energy to start the polymerization at the end of the optical fiber.

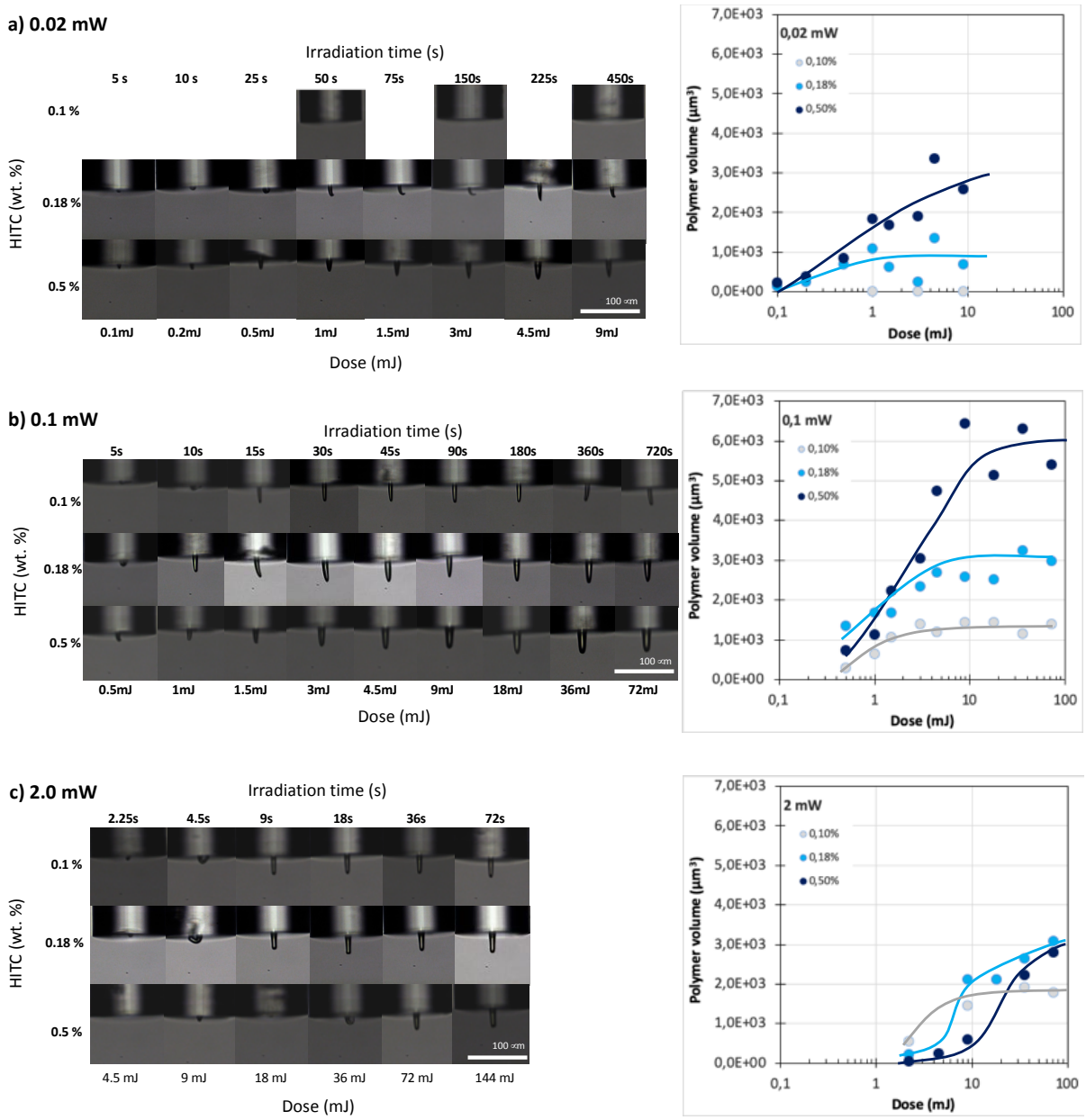

Figure 5. Impact of HITC concentration on the microfabrication process, for a) 0.02 mW, b) 0.1 mW and c) 2.0 mW. For each series, the volume of the polymer tip has been evaluated from microscopy images and plotted versus dose, assuming that the shape of the tip is a half-ellipsoide.

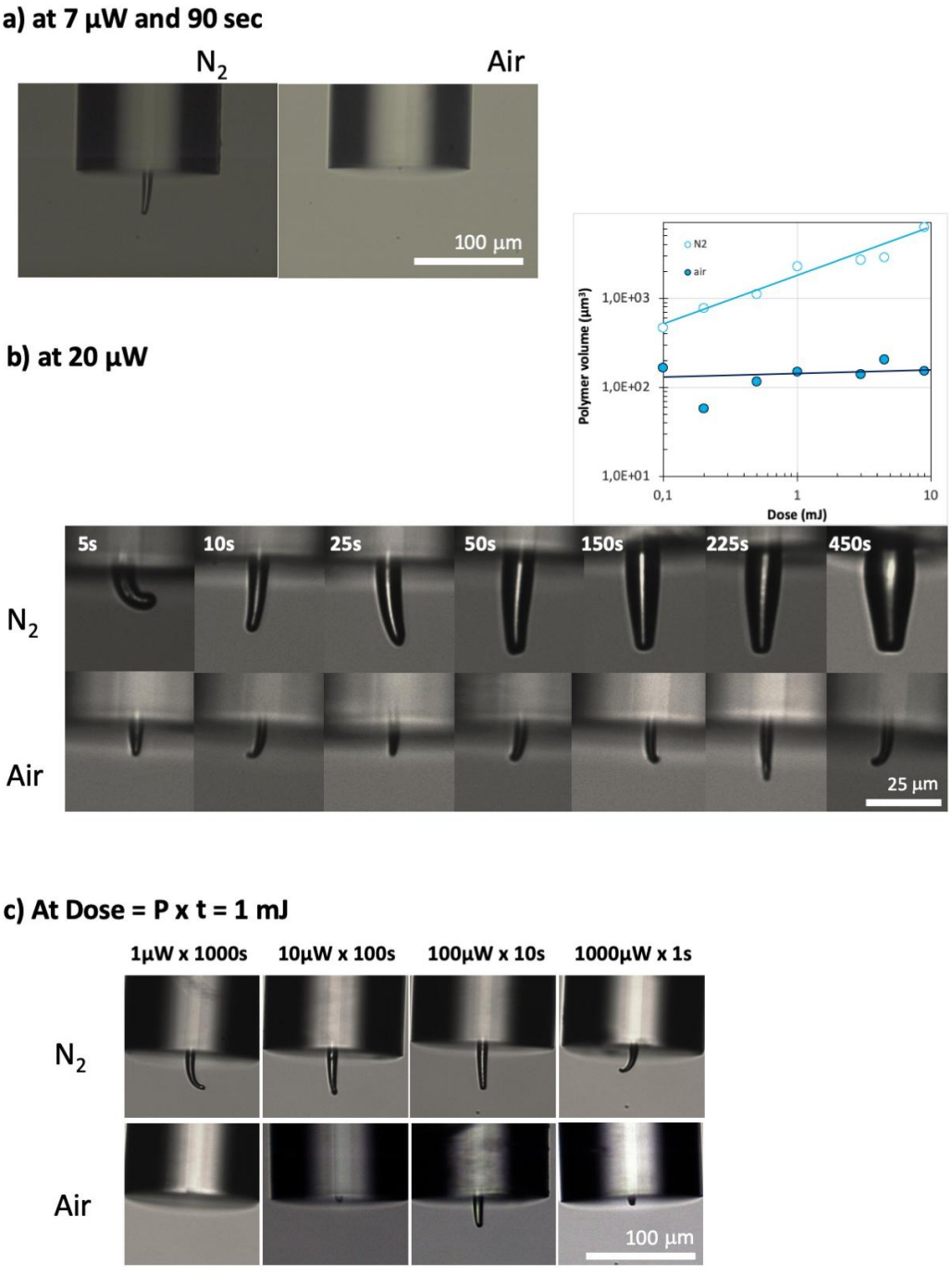

Figure 6. Influence of oxygen on the microstructuration process. a) shows the difference between well-aerated conditions and under nitrogen atmosphere (photonic conditions were chosen similar: 7 µW, 90 sec.). b) Growth dynamic of the microtip under low intensity conditions, at air and under N_2 (20 µW) and evolution of the polymerized volume as a function of the dose under air and nitrogen atmosphere. c) Comparison of the effect of intensity at a constant dose (1 mJ), under air and N_2.

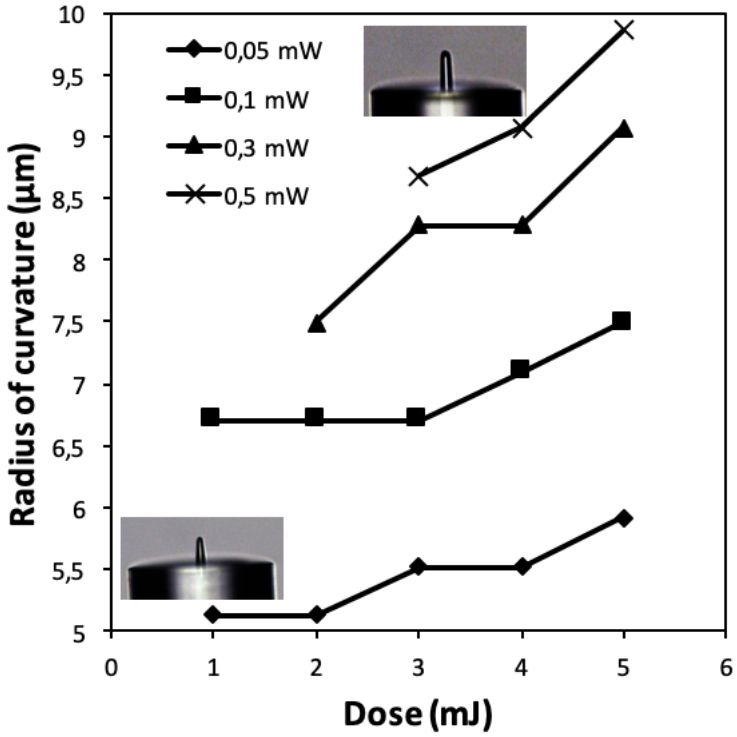

Figure 7. Evolution of the radius of curvature of the microlens with dose for several intensities ranging from 0.05 mW to 0.5 mW.

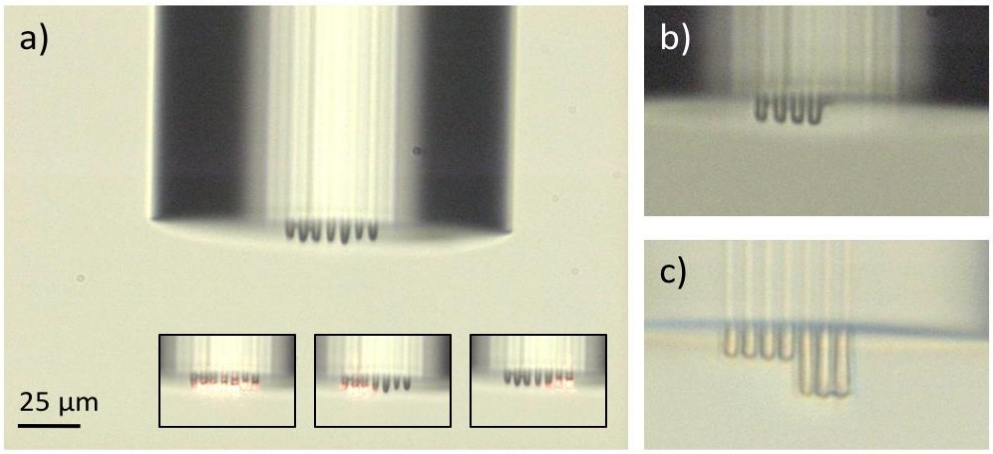

Figure 8. a) Fabrication of arrays of microlenses on multicore fiber (7 cores). Insets show the excitation using several modes to select different lenses. b) Excitation of 4 cores during fabrication, leading to 4 microlenses. c) From the same sample as in b), 3 new tips were grown using longer irradiation time.

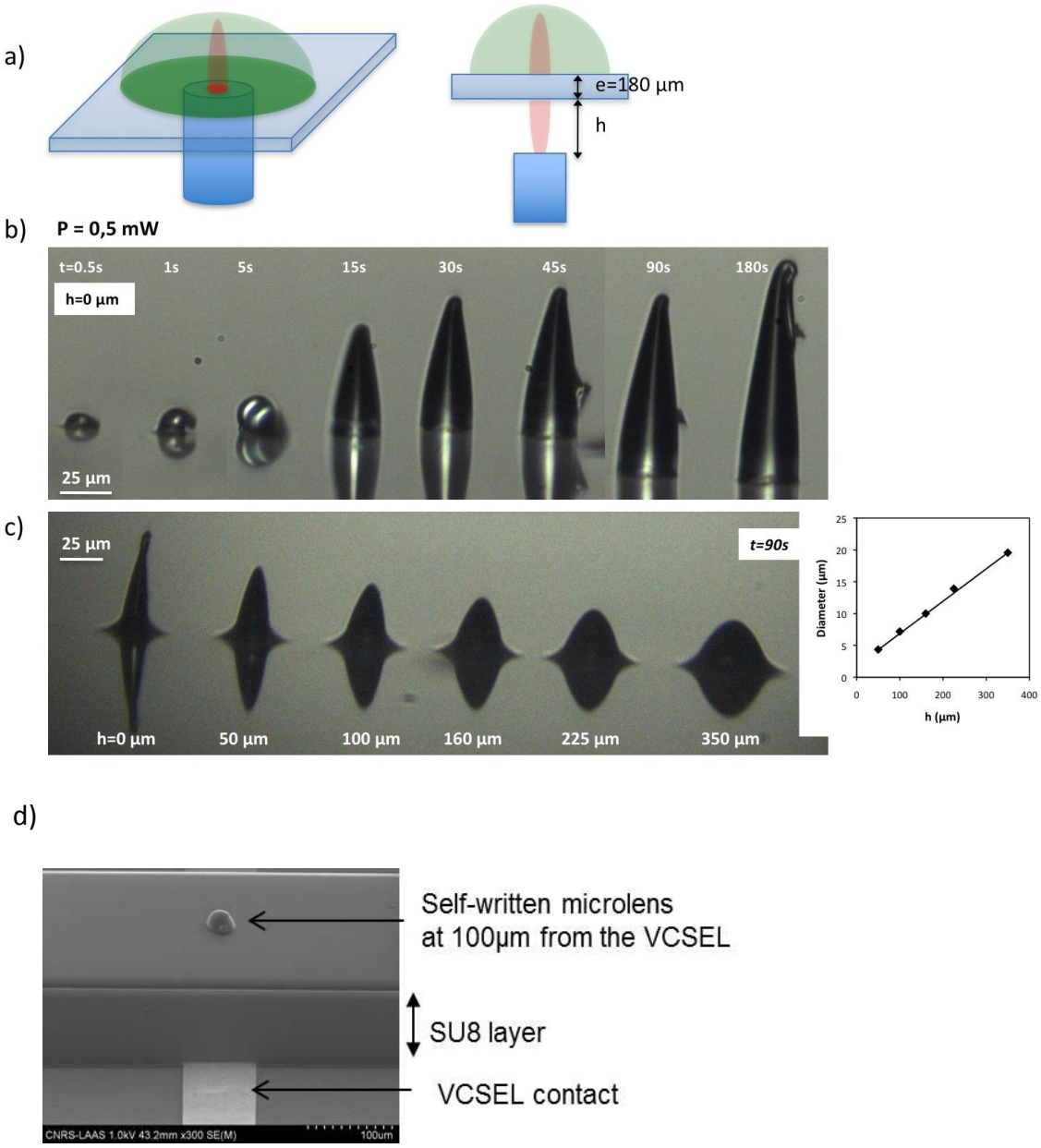

Figure 9. a) Schematic view of the experimental configuration for writing lenses on glass substrate. e is the thickness of the glass slide (180 µm), and h is the distance between the end of the fiber and the glass slide. b) Series of microlenses fabricated with P=0.5 mW and various irradiation times for h=0 µm. c) Series of microlenses fabricated with P=0.5 mW, t=90 s, and various h distance. d) Microlens on SU8 spacer (thickness 100 µm) created by the VCSEL.

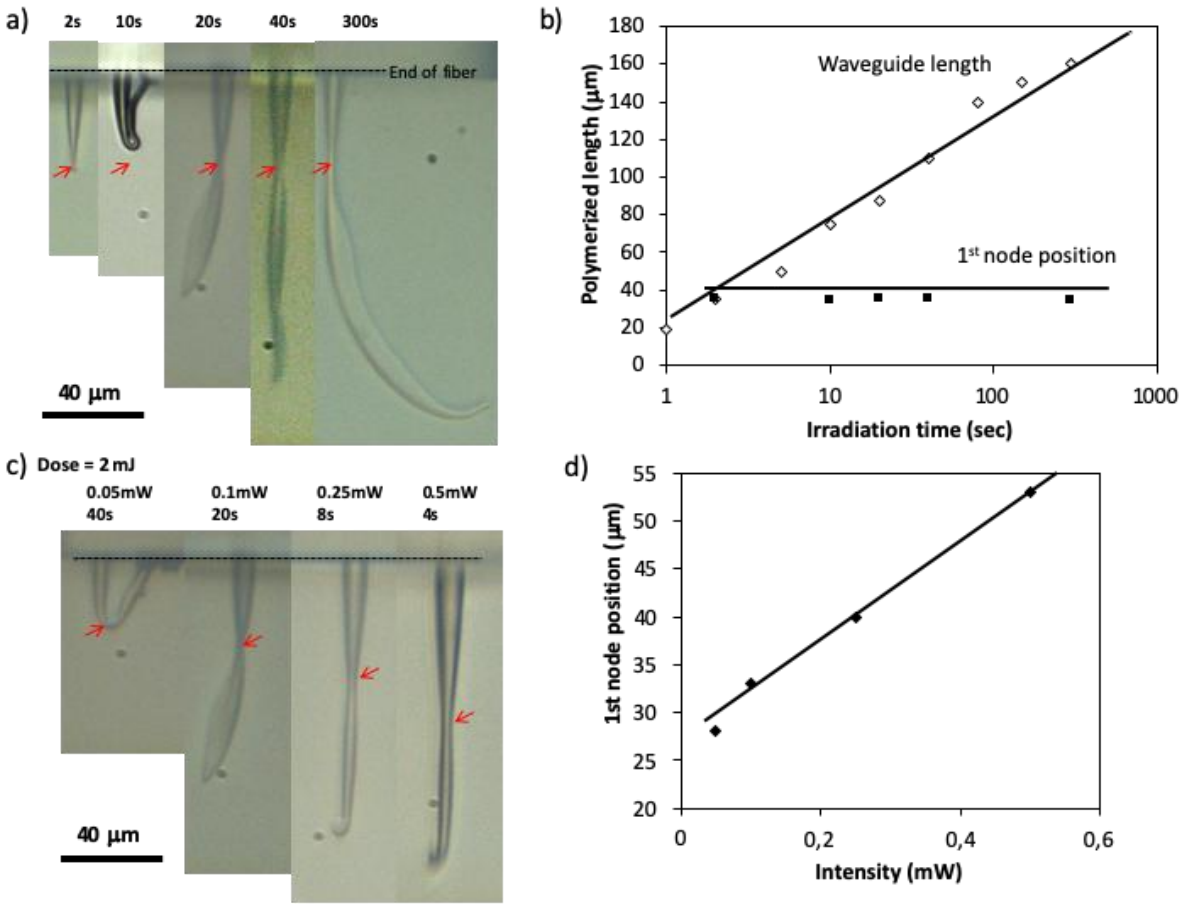

Figure 10. Building up of the waveguide on optical fiber. a) Images of waveguides for various irradiation times and for a given intensity (0.1 mW), and b) evolution of the length versus irradiation time. The red arrows show the position of the first focalisation node. c) Images and d) plot of the position of the constriction node for a given dose (2 mJ) and various intensities.

The table of contents entry

A NIR photopolymer for fabrication of micro-optical elements by direct writing in the NIR region was developed and investigated. The photosensitivity of this negative tone photoresist allows using the NIR-light source itself to start the crosslinking process, which constitutes a new approach for micro-optics integration on NIR sources. Practical examples of microlenses and waveguides implemented on single core and multiple core optical fibers, VCSELs, and glass slides are presented.

Keywords. Photopolymer, microlenses, waveguide, optical fiber, NIR

*Ihab Dika, Frédéric Diot, Véronique Bardinal, Aurélien Bruyant, Jean-Pierre Malval, Carole Ecoffet, David Barat, Benjamin Reig, Jean-Baptiste Doucet, Thierry Camps and Olivier Soppera**

NIR photoresist for micro-optics self-writing